JOURNAL OF MATERIALS SCIENCE 7 (1972) 1069–1079

Review: Scanning high-energy electron diffraction (SHEED) in materials science

M. F. TOMPSETT
Bell Telephone Laboratories Inc, Murray Hill, New Jersey, 07974, USA

The SHEED technique enables direct and rapid quantitative measurement of energy-filtered electron-diffraction intensities to be made. It may be used for structural studies of single crystals, polycrystalline films and amorphous materials. These may be examined in transmission if sufficiently thin or, otherwise, by reflection electron diffraction. In addition to conventional passive observation, structural studies of growing thin and thick films may be made during deposition. Work on all these topics is reviewed and the advantages of SHEED in each case clearly demonstrated.

1. Introduction

Scanning high-energy electron diffraction (SHEED) has now been applied to so many experimental situations that it is possible to review only a few of them in this paper, but those that are discussed should indicate its versatility in materials science. High-energy electron diffraction with photographic recording of the diffracted intensities is an established technique. The function of this paper is to describe the way in which this technique has been streamlined to give great increases in recording accuracy and sensitivity. One aspect which will be emphasized is the new freedom that the scanning technique has given in allowing the performance of *in situ* dynamic experiments, i.e., characterizing how a structure is reached in addition to the final structure.

2. Instrumentation for SHEED

There has been a long history [1] of methods for directly recording the diffracted electron intensities, but these were never engineered for wide application. The present system of scanning electron diffraction, borrowing techniques from scanning electron microscopy, was first described

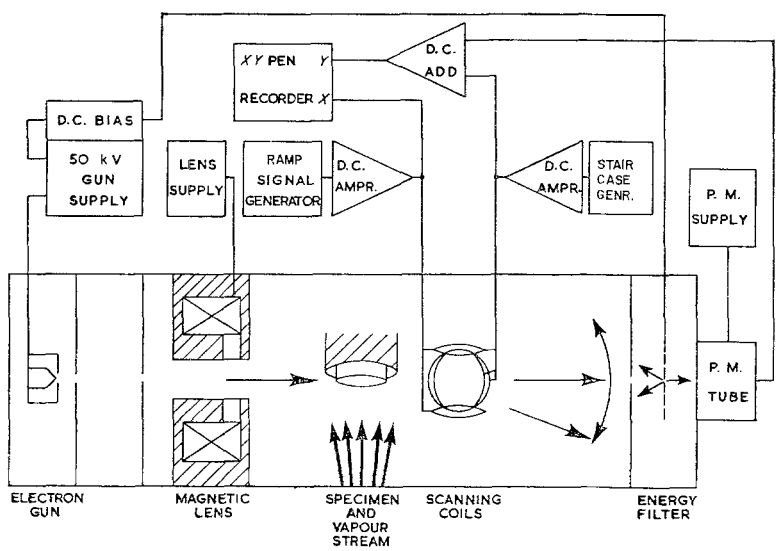

Figure 1 Schematic drawing of a scanning high-energy electron diffractometer [3].

by Grigson in 1961. Several instruments using these principles have now been built [2, 3]. The basic system is shown in Fig. 1. Electrons from an electron gun are focused by a magnetic lens onto what is the normal viewing screen, which in this case contains a small aperture. Between the lens and the screen the electron beam passes through the specimen, shown in Fig. 1 as a reflection specimen, and where the electrons are diffracted. The whole diffraction pattern is magnetically scanned across the aperture by passing current through the orthogonal scan coils just behind the specimen. Those electrons passing through the aperture at any given time

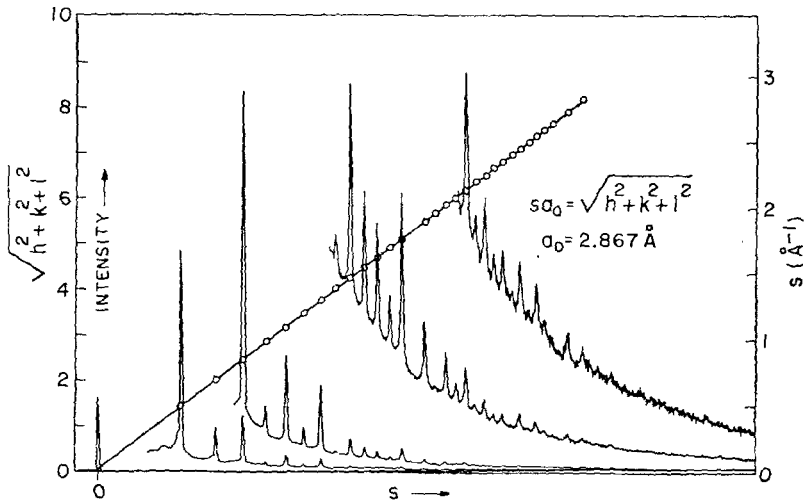

Figure 2 A simple radial scan of the energy-filtered electron-diffraction intensities from a polycrystalline film of iron deposited on a thin carbon film viewed in transmission at 30 keV. The peaks are indexed and reciprocal *d*-spacing is plotted on a vertical axis also [4].

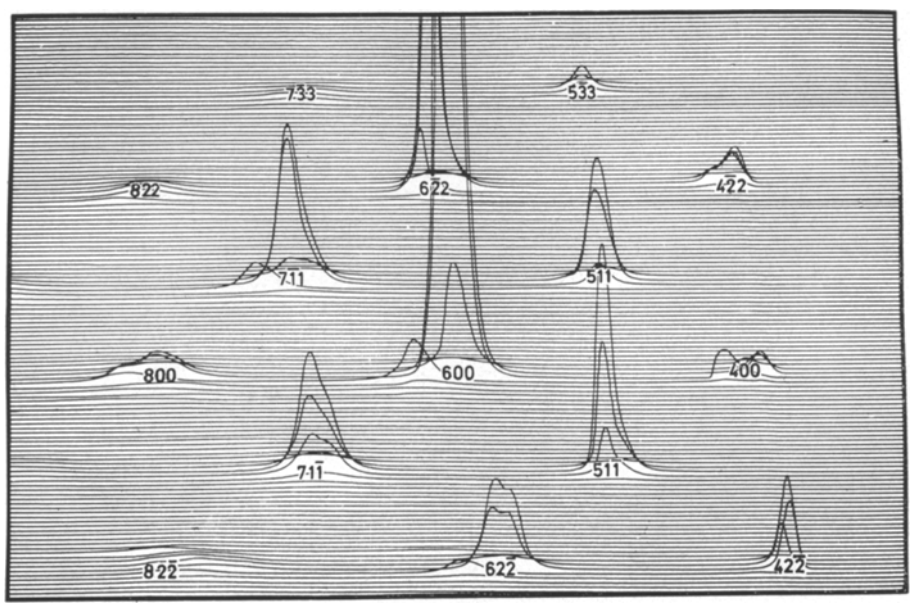

Figure 3 A three-dimensional display of the filtered diffraction pattern made by reflection of 15 keV electrons from a single crystal of GaAs. The incident beam is incident at (000) off the right hand side of the display [5].

are energy filtered, that is all electrons which have lost energy in passing through the specimen are rejected and only the elastically scattered ones accepted. The filter consists of a mesh held at a potential a few volts more positive than the electron gun potential. The resolution of a filter of this type is typically 1 in 10^4. Those electrons that penetrate the mesh are reaccelerated onto a phosphor causing scintillations which are detected with a photomultiplier tube. The output from this tube gives a current proportional to the electron intensity at a given point in the diffraction pattern.

The diffracted intensity is recorded on an X-Y pen recorder or oscilloscope as a function of the current through the scan coils. An example [4] of a simple radial scan is shown in Fig. 2. Here scans along a radius of the polycrystalline ring diffraction pattren of an evaporated iron film have been made. The radial distance is plotted on the X-axis and intensity on the Y-axis. Several scans have been made at different gain settings so that both the strongest and the weakest peaks may be displayed. The excellent scan linearity is shown in Fig. 2 where the peaks have been indexed directly on the recorder plot and the reciprocal d-spacing plotted on the vertical axis.

A two-dimensional scan may be generated and displayed as shown in Fig. 3. Voltages proportional to the currents in the X, Y scan coils are fed onto the X, Y-axes of the recorder respectively. The intensity also is added onto the Y-axis. By scanning the X current and stepping the Y current in increments such a display can be produced. The display [5] in Fig. 3 is a record of the elastically-scattered diffraction intensities from a GaAs single crystal specimen viewed in reflection and shows much more contrast than would have been the case without filtering. This display is, of course, a record of the intensities found in a section of reciprocal space of the crystal.

The scanning technique may be applied either in an instrument designed exclusively for electron diffraction studies and which may be termed an electron diffractometer, or in the transmission electron microscope. In this latter case the scan coils are normally inserted below the intermediate lens and the energy filter and detector are placed below the observation chamber [6, 7]. This extra facility is now commercially available for the electron microscope [8]. In this way accurate measurements of energy-filtered intensities as required in structure analysis and diffraction contrast studies of single-crystal films, may be obtained.

The improved accuracy of direct recording with energy filtering as compared to photographic recording arises for two reasons. The combined use of a high-gain photomultiplier tube and an X-Y recorder gives linear intensity measurements over at least six decades that is better than 0.5% accurate. This is obtainable routinely and instantly without any special calibration. The second reason arises from the elimination of the inelastically-scattered electrons, which otherwise produce broadening of the diffraction peaks and an increase in background scattering. The intensity of these incoherently scattered electrons varies as a function of the

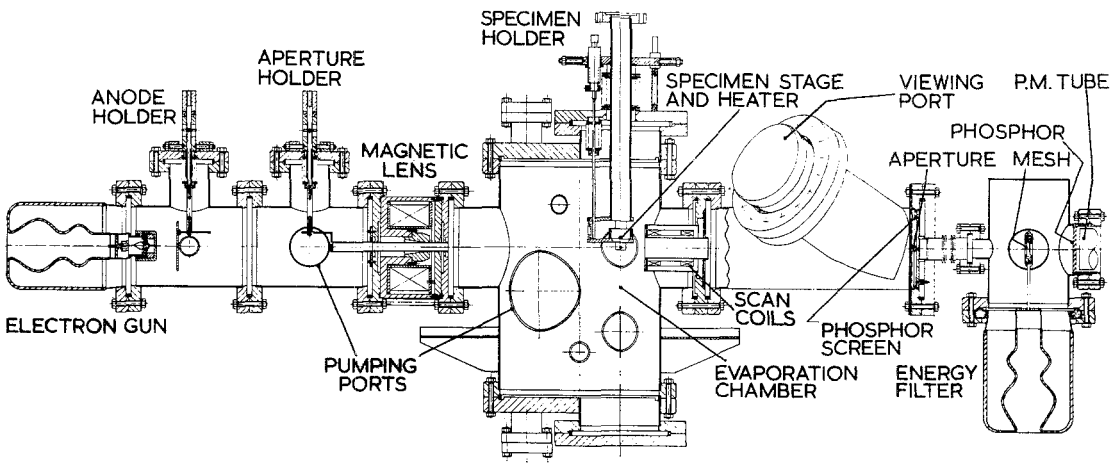

Figure 4 Section drawing of a versatile scanning high-energy electron diffractometer [3].

scattering angle and, as will be shown, can on occasions be greater than the elastically-scattered intensities. The use of unfiltered intensity data therefore leads to inaccuracies in any deductions based on theories that invariably assume elastic scattering. A computer-controlled system has been built [9] for the automatic collection of diffraction data and similar techniques could be applied to any instrument. In many cases the electron diffractometer is the preferable facility for performing structure studies on materials, as the control of the ambient and the provision of deposition facilities is much easier than in the electron microscope. All the experiments discussed in this paper have been performed in electron diffractometers.

If electron-diffraction experiments are to be accurate then a contaminant-free vacuum is required. Hydrocarbon contamination is a particular problem as it is absorbed onto a specimen and "cracked" by the electron beam to form a carbon film. This film then gives rise to additional scattering appropriate to amorphous carbon. In the case of reflection-electron diffraction from a smooth surface examined in a conventional high-vacuum system, a film of carbon several Angstroms thick can be formed in seconds and obscures the diffraction pattern of the substrate. These films are also clearly detectable on thin films viewed in transmission. Hence ultra-high vacuum construction and pumping techniques are required, even if high gas-pressure ambients are used. The cross-section of an ultra-high-vacuum electron diffractometer [3] is shown in Fig. 4. The gun and energy-filter sections are separately pumped, which enables a controlled ambient ranging from 10^{-9} to 10^{-2} torr to be produced in the specimen chamber while allowing the operation of the electron beam. This control of the ambient is invaluable in both thin film growth and surface studies. The instrument uses a horizontal electron beam and a modular ultra-high vacuum (UHV) construction. Working with UHV in the system does not impede rapid examination of specimens since a specimen airlock is used. A similar instrument is now commercially available [10].

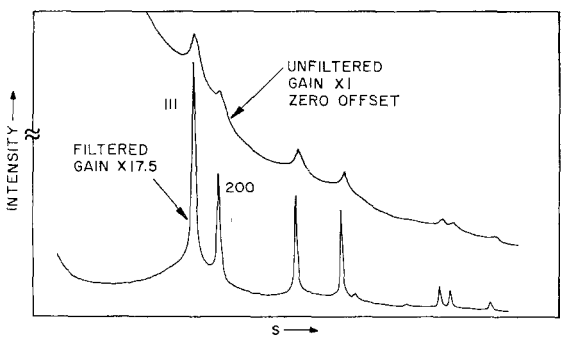

Figure 5 Diffracted intensities produced by transmission of 50 keV electrons through a 1 μm thick aluminium foil. The unfiltered and filtered profiles are shown [11].

3. Energy filtering in electron diffraction

The importance of energy filtering cannot be overemphasized. A high percentage of the diffracted electrons always suffer inelastic scatter-

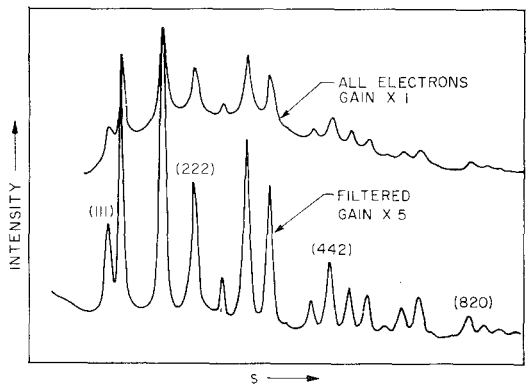

Figure 6 Electron-diffraction intensities by reflection of 20 keV electrons from MgO powder. The upper trace shows the unfiltered diffracted intensity while the lower trace shows this intensity filtered and amplified. Only electrons that have lost less than 10 eV are included after filtering in order to obtain the maximum contrast [5].

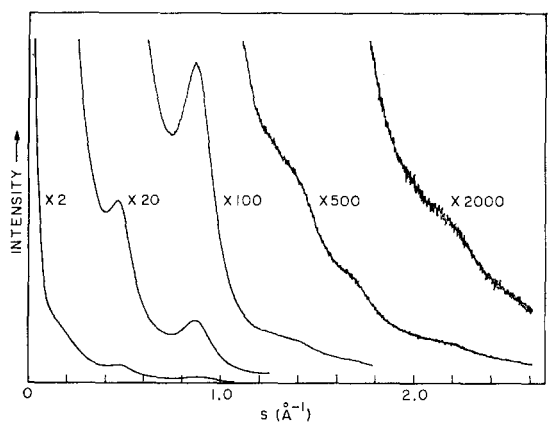

Figure 7 A simple radial scan showing the energy-filtered diffraction profiles from a carbon thin film viewed in transmission at 30 keV. The gain of the intensity channel is indicated [4].

ing, which adds a background and peak broadening to the elastically-diffracted intensities. By eliminating these electrons much higher contrast and accuracy in quantitative interpretation, which is based on elastic-scattering theory, are obtained. In diffraction through thick films, in particular, the inelastically-scattered background becomes very large. This is illustrated [11] in Fig. 5 for the case of a 1 μm thick Al foil viewed in transmission at 50 keV. The upper trace is unfiltered and should be displaced many times up the screen. It shows a negligible diffraction contrast. The lower trace shows that the diffraction pattern similar to that from a thin aluminium film has been revealed by energy filtering.

Reflection-electron diffraction has always suffered from low contrast. This is largely due to inelastic-scattering although inherently the contrast of the filtered intensity profiles will be less than that obtained by transmission through thin films. The upper profile of Fig. 6 shows the unfiltered intensity recorded in reflection from a deposit of MgO [5]. The effect of energy filtering is seen in the lower profile, in which the intensities have been filtered and displayed with increased gain. This profile shows an order of magnitude increase in contrast over the unfiltered trace.

Radial distribution function analysis provides a way of characterizing amorphous materials. Fig. 7 shows the intensity profiles in a simple radial scan for a carbon thin film viewed in transmission [4]. The necessary conditions for accurate RDF analysis of amorphous materials are met in SHEED. These involve using energy-filtered intensities, which are essential [12-14], and which have been measured as a function of angle over a wide angular range and many decades of intensity. The output of the photomultiplier tube or intensity signal could, of course, be digitized at source onto tape for immediate computation.

Fig. 8 shows how minute detail, invisible in a photographic record, can be revealed in a diffraction pattern using SHEED [15]. Fig. 8a shows a two-dimensional scan of the diffraction pattern from a single-crystal thin film of Al-4% Cu alloy viewed in transmission. The intensities are not filtered and the differing widths of the peaks, particularly that of the zero-order beam, which dominates the display, and the high background are evident. In Fig. 8b filtering has been introduced and marked peak narrowing and reduced background are evident. In Fig. 8c the intensity gain and the X-, Y-scales have been increased so that detail in the small portion indicated in the display of Fig. 8b may be seen.

4. Structures of growing thin films

The rest of this review will be concerned with the dynamic characterization of the structures of thin films grown in the diffractometer. The recording method [16] is illustrated by Fig. 9. In this case lead was evaporated onto a thin carbon substrate through which the electron beam passed in transmission mode [4]. The two sets of diffraction patterns (a) and (b) in Fig. 9 were recorded while scanning in both directions. The lowest scan in each case is the intensity due to the substrate. The mean film-thickness increments between scans in cases (a) and (b) were 1.0 and 2.7 Å respectively. In most of the cases to be described, the films are still thin enough so as to be discontinuous, and the individual islands or crystallites are separated. The beam size at the specimen is such that the beam covers many islands and the diffraction pattern is an average over these islands. The increasing contrast in the diffraction pattern arises as the crystallites become larger. In case (a) the substrate temperature was 20° C and a gradual growth of the crystallites is evident. However, in case (b) when the substrate temperature was 128° C a considerable difference is quite evident. Analysis of the structure using the radial-distribution function obtained from the diffracted intensities shows [4] that the islands formed initially are supercooled droplets of lead, which, at a critical size, crystallize and instantaneously produce the sharp diffraction peaks which appear in the upper traces.

Another type of phase change is demonstrated in Fig. 10 which shows the growth of an iron film deposited onto carbon and viewed in transmission [4]. The presence of an amorphous layer is evident from the initial intensity profiles but at a critical film thickness, around 25Å, most of this amorphous material converts to the normal bcc structure. This conversion is shown by the abrupt appearance of sharp peaks in the intensity profiles, indicating that relatively large crystallites have formed instantaneously. This effect has also been observed in other metals [17]. With the high recording speeds, several scans per second, possible in SHEED [2], many phase change processes are observable using this technique.

The large working space available in a

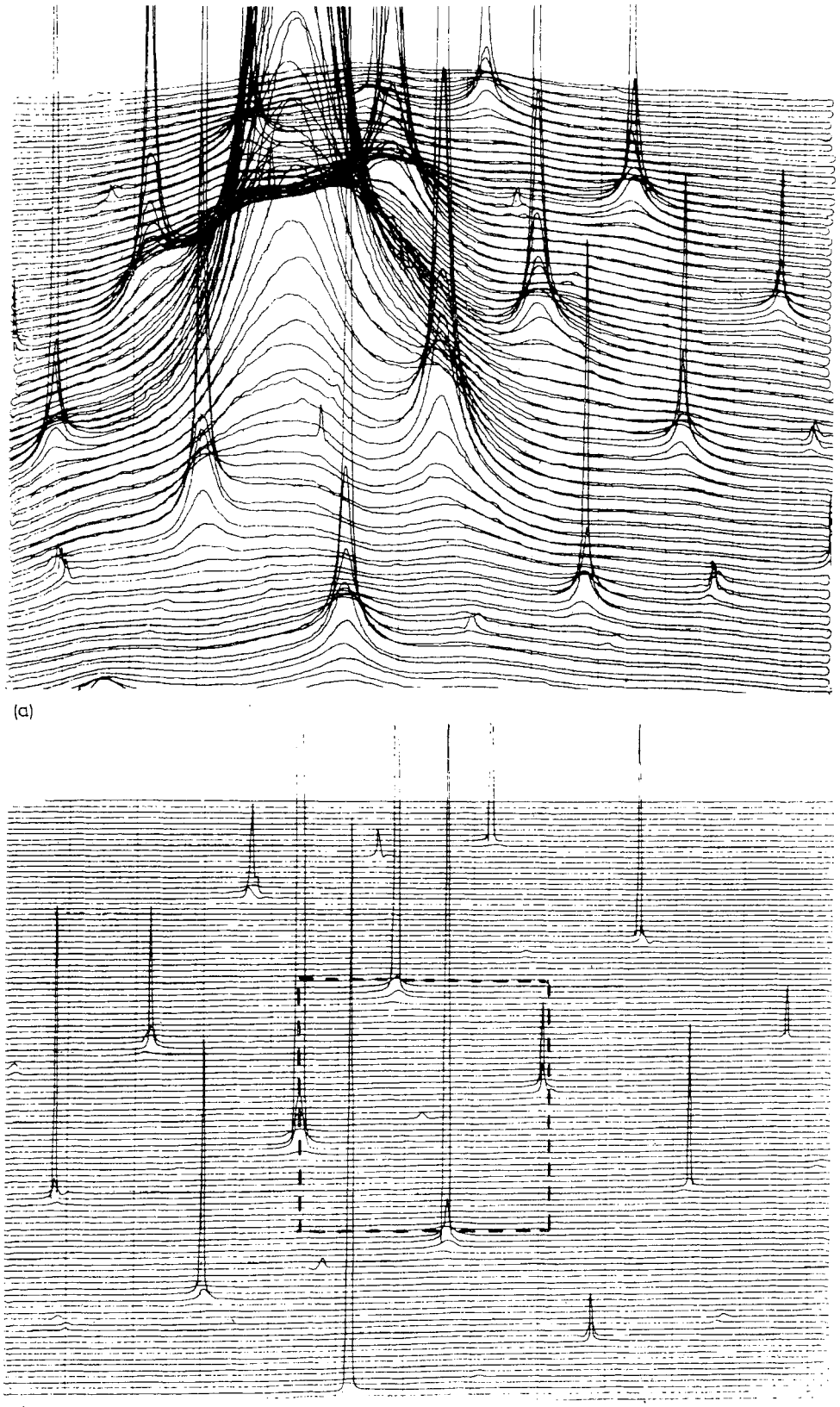

Figure 8

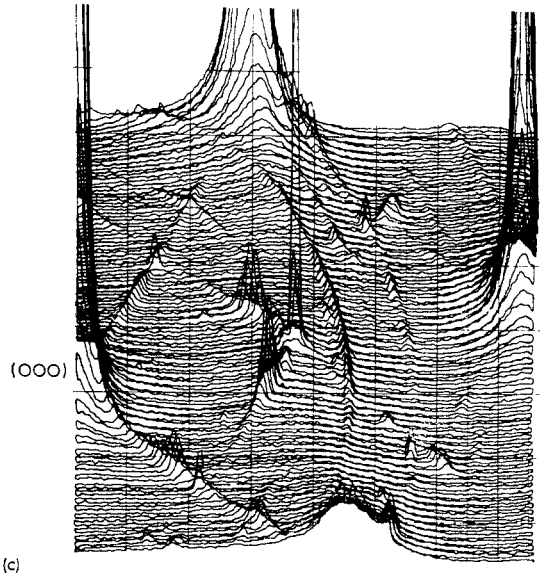

Figure 8 Three-dimensional displays of the diffraction patterns produced by transmission through a single crystal Al-4% Cu film. (a) Unfiltered, (b) filtered, and (c) the intensity gain and the *X*-, *Y*-scales increased for that portion of filtered display indicated in (b).

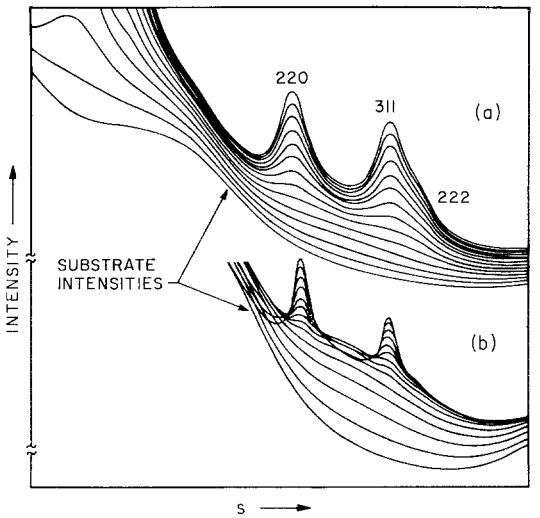

Figure 9 Simple radial scans of the energy-filtered diffraction patterns from a film of lead continuously deposited onto a carbon substrate and viewed in transmission. (a) The substrate temperature was 20°C and the film-thickness increments between scans are 1Å. (b) The substrate temperature was 128°C and the film-thickness increments are 2.7Å [4].

scanning electron diffractometer allows bulky specimen holders and specimen preparation facilities to be used. For example a liquid-helium cooled substrate held in a cryostat has been inserted into the specimen chamber of an electron diffractometer. Fig. 11 shows the diffraction pattern obtained from solid hydrogen condensed on the substrate and viewed in transmission [15]. Two structures were detected on different parts of the film and the intensity profiles are shown recorded and indexed in Fig. 11.

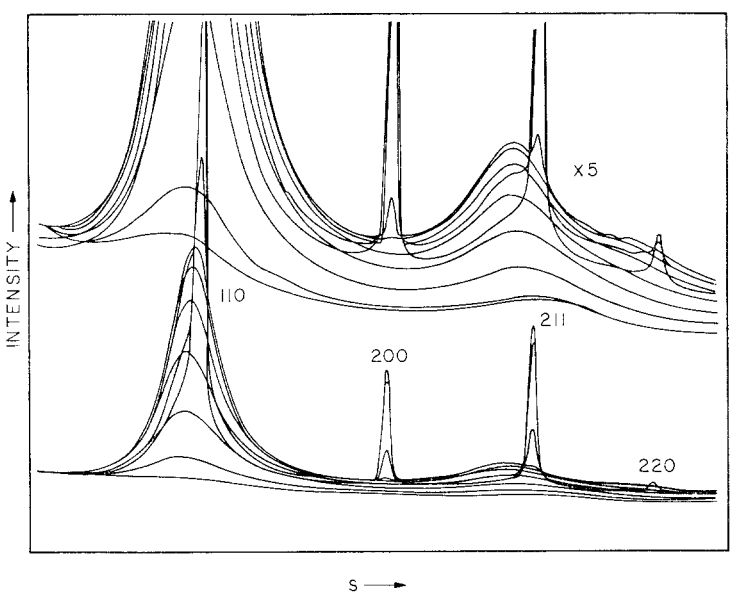

Figure 10 Simple radial scans of the diffracted intensities from a film of iron continuously deposited onto a thin carbon substrate at 25°C. The film-thickness increments between scans is 5Å [4].

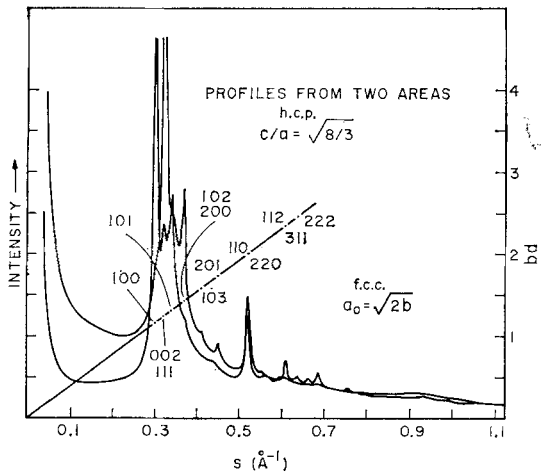

Figure 11 Simple radial scans of the diffracted intensities from two areas of a film of hydrogen condensed onto a carbon substrate at 5 K. Each area shows a different structure, one is hcp and the other fcc, both of which are indexed [15].

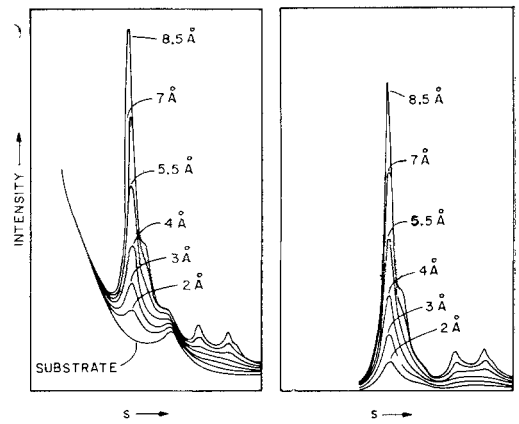

Figure 12 (a) Shows the intensity profiles from a lead film growth onto a carbon substrate at 25°C. (b) Shows the profiles after subtracting the substrate intensity. The film thicknesses in each case are shown [14].

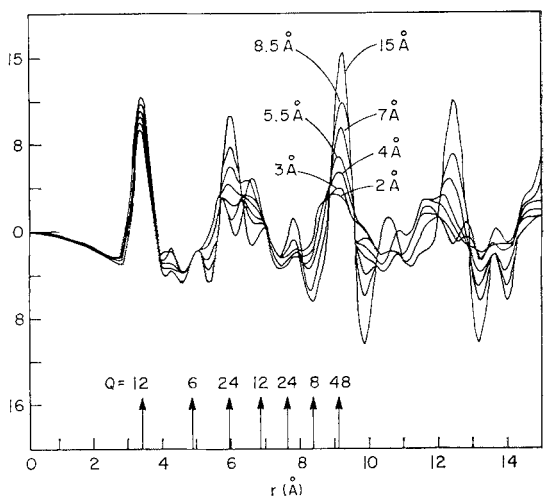

Figure 13 Shows the relative radial-distribution functions of the lead films whose intensity profiles are shown in Fig. 12 [14].

One topic of continued interest in studying the growth of thin films is characterization of the structures of the smallest crystallites. This may be done with considerable accuracy using SHEED. Fig. 12a shows a section of the intensity profiles from a lead film growth seen at the successive thicknesses indicated [14]. The lowest lying profile is that of the substrate only and this is subtracted from the other profiles to give the metal-only profiles shown in Fig. 12b. These profiles are digitized and put through a radial distribution function analysis or Fourier transform process, which produces an RDF or plot of the mean radial density of atoms from any given atom in the material The RDF's of the crystallite structure at each mean film thickness are shown in Fig. 13. The evolution of the longer range order as the islands grow is clearly shown. With the structure characterized by the RDF, the actual structure can be elucidated by comparisons with the computed RDF's of model structures. The best fit in the case of the 2Å mean thickness film was found [14] to be that of a 55 atom icosahedral crystallite.

5. Small angle electron diffraction of ultra-thin films

Small-angle electron diffraction is a powerful tool in the study of ultra-thin films. Such films are discontinuous and give rise to marked diffraction effects at small angles. These effects which appear at small angles in the equivalent d-spacing range of 20 to 100 Å arise from the form factor of the islands and the interisland spacings. Energy filtering is essential [18, 19] to the revelation of detail such as is shown in Fig. 14. (This is equally true when crystals with long d-spacings are studied [20]. The small-angle intensity profiles for several ultra-thin films, all less than a monolayer thick, are shown in Fig. 15. A mathematical expression for the diffracted intensity has been derived [19, 21] and may be fitted by the method of least squares to the

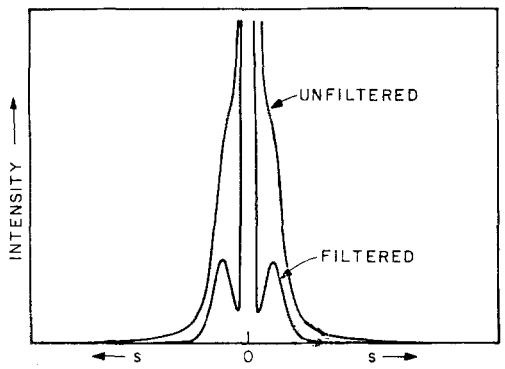

Figure 14 Small-angle energy-filtered and unfiltered diffracted-intensity profiles from a 10Å thick film of silver on a 200Å thick carbon substrate [19].

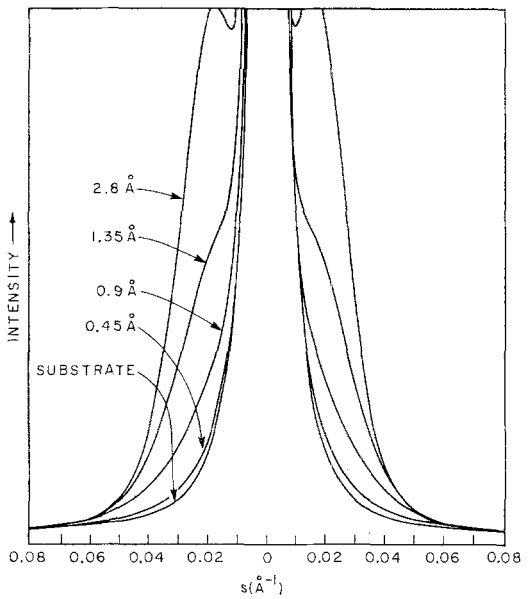

Figure 15 Small-angle diffraction profiles from silver deposited into carbon at the mean thickness increments shown. The top profile corresponds to a mean monolayer coverage of silver atoms [21].

experimental intensities. This enables the mean radius-of-gyration of the island separation, and other parameters, to be computed. The expression is verified by several correlations [21], particularly by the linear relationship obtained between the computed number of atoms and the mean film thickness. The results of computer-curve fitting are shown in Fig. 16. The continuous lines are experimental and the points represent the "best fit" of the expression referred to above. The smallest islands measured in this way had a mean radius-of-gyration of only 11 ± 1Å.

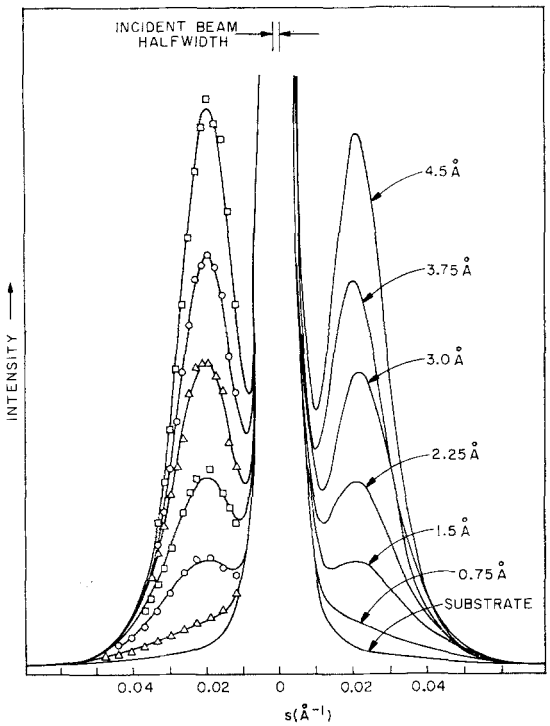

Figure 16 Small-angle electron diffraction profiles of silver deposited onto carbon. The plotted points are the results of computer curve fitting [21].

Additional inaccuracy than that indicated, possibly arises from the assumption of the particular statistical model of island size and distribution used in the calculation of the electron scattering. That this technique can measure such small islands indicates that its sensitivity is better than that of direct imaging in the electron microscope and has the advantage of generating quantitative data on the earliest stages of crystal growth. This fact also means that only one instrument, the electron diffractometer, is required to derive both the structure and form of these thin films. In addition, the control of the ambient and the provision of deposition facilities is much easier in the diffractometer than in the electron microscope.

6. Engineering a thin film structure

The final section of this paper will be concerned with observing the later stages of film growth using reflection-electron diffraction, and engineering a required structure in a film. The material studied was lead monoxide which was known to be a semiconductor suitable for application in a television camera tube. It exists in a tetragonal and an orthorhombic form both

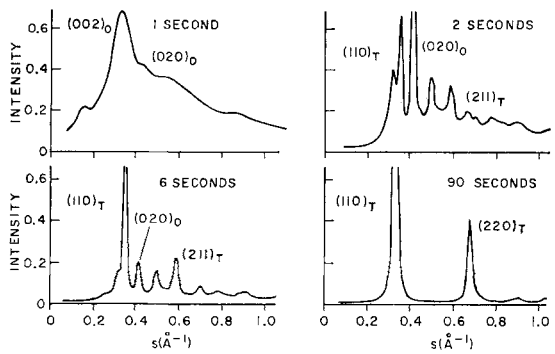

Figure 17 Diffraction profiles of a discontinuous growth of PbO deposited at 1000Å sec^{-1} onto an aluminium substrate in 10^{-3} torr H_2O-O_2 and viewed in reflection mode [22.]

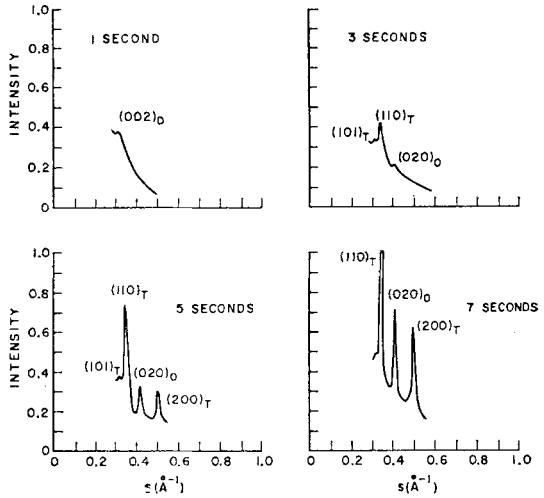

Figure 18 Diffraction profiles of a continuous growth of PbO deposited at 400Å sec^{-1} onto an aluminium substrate in 10^{-2} torr H_2O-O_2. Each scan took 1 sec to make and was made simultaneously with the deposition [22].

stable at room temperature. From the known single-crystal properties, the structure required for the application could be specified. The problem was then to find deposition conditions such that this structure was produced. The UHV diffractometer [3] already described was used for *in situ* growth studies [22]. Fig. 17 shows a discontinuous growth at a very high deposition rate (1000Å sec^{-1}) in a gas ambient of 1×10^{-2} torr oxygen and water. After 1 sec of evaporation, the structure consists of orthorhombic platelets lying on the substrate. As growth continued, a secondary nucleation process occurred and new platelets of both phases appeared. A tertiary nucleation on the faces of these platelets caused an evolution to an all-tetragonal film with a high degree of preferred orientation. The SHEED pattern for this final stage, after deposition for 90 sec and when the film is 9 μm thick, is shown at the lower right of Fig. 17. These nucleation processes are strongly dependent on the gas ambient, the deposition rate and the temperature of the substrate. The results of changing these factors are large differences in the relative amounts and orientations of the two lead oxide phases in films of similar thickness. Preferred orientations of the films were precisely determined by carrying out two-dimensional scans. Finally, continuous deposition with simultaneous recording of the diffraction pattern is possible even at the high gas pressures used and gave yet different results, as is shown by Fig. 18. These scans took only 1 sec each to record. After observing many such growth sequences made under various conditions in a period of only a few weeks, the various growth processes and the factors affecting them could be described. In addition it was determined how a required film structure for the particular application could be produced. The high throughput of experiments, plus the ability to study films ranging from ultrathin to very thick, are features available with SHEED which are extremely important in any film growth study.

7. Summary

SHEED is a new technique for materials characterization. The necessary instrumentation and techniques are now well established and a versatile SHEED instrument is commercially available [10]. Hence it behoves materials scientists to consider its application in their own fields of interest. The considerable advantages of energy filtering and direct recording over photographic electron diffraction have been clearly demonstrated. In addition the technique of electron diffraction is much more sensitive and faster than X-ray diffraction. The particular capabilities of characterizing thin films have been shown. The facility to record sequences of diffraction patterns also enables changing structures and hence the processes involved in reaching a final structure to be characterized. Finally, a new form of materials engineering has been introduced in which the electron diffractometer acts as a thin film workshop for the fabrication of thin films with a specified structure. This suggests the possibility of being able to determine how to make thin films having some of the properties,

for example a polar axis, that are normally associated with single crystals.

References

1. C. W. B. GRIGSON, "Studies of Polycrystalline Films by Electron Beams", Advances in Electronics and Electron Physics, Suppl. **4**; "Electron Beam and Laser Beam Technology", Ed. L. Marton and A. B. El Kareh (Academic Press, New York and London, 1969).
2. C. W. B. GRIGSON and P. I. TILLETT, *Int. J. Electron*, **24** (1968) 101.
3. M. F. TOMPSETT, D. E. SEDGEWICK, and J. ST. NOBLE, *J. Sci. Instrum. (J. Phys. E.)* Series 2, **2** (1969) 587.
4. M. B. HERITAGE, "Growth Studies on Thin Films Using Scanning Electron Diffraction", Univ. of Cambridge Ph.D. Diss., 1968.
5. M. F. TOMPSETT and C. W. B. GRIGSON, *Nature*, **206** (1965) 923.
6. G. R. BRADBURY, *J. Appl. Cryst.* **2** (1969) 254.
7. J. F. GRACZYK and S. C. MOSS, *Rev. Sci. Instrum.* **40** (1969) 424.
8. A.E.I. Ltd. (Harlow, England).
9. R. J. HOLMES, I. E. POLLARD, and C. J. RYAN, *J. Appl. Cryst.* **3** (1970) 200.
10. Vacuum Generators Ltd, Charlwoods Road, East Grinstead, Sussex, England. Marketed in the USA by Veeco, Inc.
11. C. W. B. GRIGSON and P. I. TILLETT, *Nature* **215** (1967) 617.
12. C. W. B. GRIGSON and M. F. TOMPSETT, *Nature* **210** (1966) 86.
13. D. B. DOVE, M. B. HERITAGE, K. L. CHOPRA, and S. K. BAHL, *Appl. Phys. Letters* **16** (1970) 138.
14. P. I. TILLETT and M. B. HERITAGE, *J. Phys. D: Appl. Phys.* **4** (1971) 773.
15. P. I. TILLETT, "Scanning Electron Diffraction at Cryogenic Temperatures", Univ. of Cambridge, Ph.D Diss. 1969.
16. C. W. B. GRIGSON and D. B. DOVE, *J. Vac. Sci. and Tech.* **3** (1966) 120.
17. P. N. DENBIGH and R. B. MARCUS, *J. Appl. Phys.* **37** (1966) 4325.
18. P. N. DENBIGH and D. B. DOVE, *J. Appl. Phys.* **38** (1967) 99.
19. M. F. TOMPSETT, M. B. HERITAGE, and C. W. B. GRIGSON, *Nature* **215** (1967) 498.
20. M. F. TOMPSETT, "Reflection Scanning Electron Diffraction", Univ. of Cambridge Ph.D. Diss. 1966.
21. M. B. HERITAGE and M. F. TOMPSETT, *J. Appl. Phys.* **41** (1970) 407.
22. M. F. TOMPSETT and J. ST. NOBLE, *Thin Solid Films* **5** (1970) 81.

Received 10 January and accepted 15 February 1972.